Interplay of primary bovine lymphocytes and Mycobacterium avium subsp. paratuberculosis shows distinctly different proteome changes and immune pathways in host-pathogen interaction

Kristina J.H. Kleinwort[1], Stefanie M. Hauck[2], Roxane L. Degroote[1], Karina Lutterberg[1], Armin M. Scholz[3], Christina Hölzel[4,5], Erwin P. Märtlbauer[4], Cornelia A. Deeg[1]*

[1] Chair of Animal Physiology, Department of Veterinary Sciences, LMU Munich, Veterinärstraße 13, D-80539 Munich, Germany;

[2] Research Unit for Protein Science, Helmholtz Zentrum Munich, German Research Center for Environmental Health GmbH, Munich, Germany

[3] Livestock Center of the Faculty of Veterinary Medicine, LMU Munich, Oberschleißheim, Germany

[4] Chair of Hygiene and Technology of Milk, Department of Veterinary Sciences, LMU Munich, Schönleutnerstr 8, D-85764 Oberschleißheim, Germany;

[5] Institute of Animal Breeding and Husbandry, Faculty of Agricultural and Nutritional Sciences, CAU Kiel, Hermann-Rodewald-Str. 6, 24098 Kiel, Germany;

*** Correspondence:**
Cornelia A. Deeg (Cornelia.Deeg@lmu.de)

Keywords: *Mycobacterium avium* subsp. *paratuberculosis*, exoproteome, immune capacity, IL12, CNOT, GroEL1, DnaK, ShinyGO

Abstract

Pathogen exoproteome and host secretome are essential for deeper understanding of host-pathogen interaction mechanisms. *Mycobacterium avium* subsp. *paratuberculosis* (MAP) is a pathogen causing paratuberculosis, a chronic granulomatous enteritis in cattle and small ruminants, resulting in severe diarrhoea, emaciation and decreased milk production. During the long asymptomatic subclinical stage, high numbers of MAP are excreted. Since MAP can survive many of the standard techniques of food decontamination (e.g. pasteurization), viable MAP are regularly found in pasteurized milk and also in dried dairy products like powdered infant formula. MAP is currently discussed in association with inflammatory bowel diseases like Crohn's disease and ulcerative colitis in man; a causal association, however, is not proven to date.

In order to gain more knowledge on the interplay of the pathogen MAP with the host-immune system and identify crucial networks in host-pathogen communication, we analysed MAP and its interaction with peripheral blood lymphocytes (PBL) from cattle with different immune response (control PBL and ID PBL) through their exoproteome/secretome.

With differential proteome analyses and mass spectrometry, we detected changed protein abundances in MAP and PBL exoproteome/secretome after co-incubation. MAP exoproteome showed higher levels of either GroEL1 or DnaK, depending on immune capacity status of host PBL used for co-cultivation. PBL secretome was further analysed using bioinformatics and results indicated different biological pathways enhanced in hosts with different immune capacities. Interestingly, we found two major regulated networks in control PBL and one distinct major network in ID PBL after co-cultivation with MAP.

The understanding of MAPs interplay with the immune system is a world-wide goal of infectiologists and food microbiologists who urgently need functional data in order to allow substantiated risk assessment of foodborne bacteria such as MAP.

1 Introduction

Mycobacterium avium subsp. *paratuberculosis* (MAP) is a critical pathogen for cattle and small ruminants, causing paratuberculosis with decreased milk production and, in some animals, excessive loss of weight (Yamamoto et al., 2018). Paratuberculosis, also referred to as Johne's disease, is world-wide endemic; no country or region has been found to be free of this disease (Li et al., 2016). Affected ruminants go through a long asymptomatic subclinical phase in which infection cannot reliably be detected by standard diagnostic tests (Hobmaier et al., 2019; Li et al., 2017). These subclinically infected animals can already shed MAP, thereby contaminating dairy products or meat (Sweeney, 2011). Diseased animals were shown to shed high numbers of MAP (Machado et al., 2018). Since viable MAP were found in pasteurized milk (Gerrard et al., 2018) and in dried dairy products like powdered infant formula (Botsaris et al., 2016), MAP are discussed as foodborne pathogens.

A similar pathology in the intestinal tissue of patients with intestinal tuberculosis and paratuberculosis was described more than a century ago. Recently, an association between MAP and Crohn’s disease was shown, initiating a discussion about a possible relationship of MAP in Crohn`s pathogenesis (Alcedo et al., 2016). Johne`s and Crohn`s disease share clinical and histopathological similarities, MAP can survive standard pasteurization procedures and MAP antibodies can be detected in Crohn`s patients, where macrolide antibiotics ameliorate disease (Kuenstner et al., 2017). In contrast, genotypes of MAP isolated from cattle and man are different, there is a lack of evidence for uptake of contaminated food in respective patients and MAP cannot consistently be isolated from Crohn`s disease patients (Mendoza et al., 2009). Neither in cattle, nor in humans MAP is transmitted from mother to child during pregnancy. But although MAP was detected widespread in many farms and different countries, the incidence of Johne`s disease in ruminants is marginal (Sergeant et al., 2019). Bacteria can survive for 2–10 years without causing obvious symptoms of infection in cows (Hermon-Taylor, 2000). As seen in cattle farms, susceptibility to MAP infection differs in human populations (Eslami et al., 2019). This points to a complex disease in which several pathogens, environmental factors and an inappropriate immune response in genetically susceptible hosts participate in the cause of disease (Eslami et al., 2019). Only little is known about the host-pathogen interaction of MAP and the immune system of its hosts (Davis, 2015). Functional differences in these responses could lead to aberrant reactions in susceptible hosts (Davis, 2015).

Recently, we detected a functionally different immune capacity in 22% of cows from different herds in Germany using differential proteome analyses (Lutterberg et al., 2018). These immune deviant (ID) cows differ in their constitutive immune proteome and they regulate different master immune regulators upon polyclonal immune cell stimulation. The phenotype is functionally correlated with an increased prevalence of mastitis, indicating an impact on the ability to fight infections (Lutterberg et al., 2018).

All living microorganisms are exposed to changing environmental parameters that define their habitats. Bacteria sense environmental changes and react to it with various stress response mechanisms (Guo and Gross, 2014). To gain information about the pathogenic mechanisms of MAP and how they respond to different immune response signals of their hosts, we analysed the changes in the proteomes of MAP after co-incubation with primary peripheral blood derived leukocytes (PBL) of control and ID cows. Since the aim of this study was a better understanding of the host-pathogen response, we analysed the exoproteomes of MAP and the bovine peripheral blood derived lymphocytes.

The term exoproteome describes the protein content that can be found in the extracellular proximity of a given biological system (Armengaud et al., 2012). These proteins arise from cellular secretion, other protein export mechanisms or cell lysis, but only the most stable proteins in this environment will remain abundant (Armengaud et al., 2012). These proteins play roles in the organism's survival in extreme habitats such as saline environments (Rubiano-Labrador et al., 2015). Investigating the exoproteome of the pathogen and the secretome of PBL provides expanded coverage of the repertoire of proteins secreted in the stress response of MAP to different immune responses and this is essential for understanding respective mechanisms. Accordingly, this study aimed at providing a better understanding of the interplay of *Mycobacterium avium* subsp. *paratuberculosis* (MAP) with the immune system on proteome level to identify the complex network of proteins involved in host-foodborne bacteria communication.

2 Material and methods

2.1. *Mycobacterium avium* subsp. *paratuberculosis* (MAP)

The bacterial strain used in these experiments was *Mycobacterium avium* subsp. *paratuberculosis* (DSM 44133), purchased from German Collection of Microorganisms and Cell Cultures (DSMZ, Braunschweig, Germany). MAP were grown on Herrold`s egg yolk agar (HEYM) (BD Biosciences, Heidelberg, Germany) for four weeks prior to harvesting for the co-incubation experiment. MAP were yielded through rinsing the agar of the cultivation tubes with phosphate buffered saline (PBS) and gentle scratching.

2.2. PBL isolation of control and immune deviant cows

Blood samples of cows were collected in tubes supplemented with 25.000 I.U. heparin. Blood was then diluted 1:2 with PBS pH 7.2 and subsequently layered on density gradient separating solution (Pancoll; PanBiotech, Aidenbach, Germany). After density gradient centrifugation (room temperature, 290 × g, 25 min, brake off), PBL were obtained from intermediate phase. Cells were then washed 3x in PBS (4°C). Withdrawal of blood was permitted by the local authority Regierung von Oberbayern, Munich, permit no. 55.2-1-54-2532.3-22-12. For determination of control or ID status, PBL were tested in *in vitro* proliferation assays as described (Lutterberg et al., 2018). Respective animals were tested at least 11 times, before being assigned to control or ID status. The animals were from a MAP-free farm and were tested negative for MAP antibodies and no MAP were detected in culture from feces.

2.3. Co-cultivation of MAP with primary bovine PBL

Primary bovine PBL ($2x10^7$) of control and ID cows were cultivated in 6 well plates in 3 ml RPMI each. 15 µg of live MAP were added for 48 h to one well, control wells were not infected. After 48 h, three technical replicates per experiment were centrifuged for 10 min at 350 x g and the supernatants were filtered through 0,5 µm filters (= exoproteome) and stored at -20°C until filter aided sample preparation (FASP). Cell pellets were lysed and total protein content measured with Bradford assay.

2.4. Proteolysis and LC-MS/MS mass spectrometry

10µg total protein was digested with LysC and trypsin by filter-aided sample preparation (FASP) as described (Grosche et al., 2016). Acidified eluted peptides were analysed in the data-dependent mode on a Q Exactive HF mass spectrometer (Thermo Fisher Scientific, Bremen, Germany) online coupled to a UItimate 3000 RSLC nano-HPLC (Dionex). Samples were automatically injected and loaded onto the C18 trap column and after 5 min eluted and separated on the C18 analytical column (75µm

IDx15cm, Acclaim PepMAP 100 C18. 100Å/size, LC Packings, Thermo Fisher Scientific, Bremen, Germany) by a 90min non-linear acetonitrile gradient at a flow rate of 250 nl/min. MS spectra were recorded at a resolution of 60000 and after each MS1 cycle, the 10 most abundant peptide ions were selected for fragmentation.

2.5 Protein identification and label-free quantification

Acquired MS spectra were imported into Progenesis software (version 2.5 Nonlinear Dynamics, Waters) and analyzed as previously described (Hauck et al., 2012; Hauck et al., 2017). After alignment, peak picking, exclusion of features with charge state of 1 and > 7 and normalization, spectra were exported as Mascot Generic files and searched against a database containing all entries of *Mycobacterium avium* subspecies *paratuberculosis* from NCBI Protein database combined with the Ensembl bovine database (version 80) with Mascot (Matrix Science, Version 2.5.1). Search parameters used were 10 ppm peptide mass tolerance, 20 mmu fragment mass tolerance, one missed cleavage allowed, carbamidomethylation was set as fixed modification, and methionine oxidation and deamidation of asparagine and glutamine as variable modifications. Mascot integrated decoy database search was set to a false discovery rate (FDR) of 1% when searching was performed on the concatenated mgf files with a percolator ion score cut-off of 13 and an appropriate significance threshold p. Peptide assignment was reimported to Progenesis Software. All unique peptides allocated to a protein were considered for quantification. Proteins with a ratio of at least five-fold in normalized abundance between control and ID or samples were defined as differentially expressed.

2.6. Enriched pathway analyses

Abundances of the identified proteins were defined as differentially expressed based on the threshold of protein abundance ratio of ≥1.5 and their assignement to MAP or bovine exoproteome. Venn diagram was made with open source tool: http://bioinformatics.psb.ugent.be/webtools/Venn/. The protein–protein interaction network of differentially-accumulated proteins was analysed with GeneRanker of Genomatix Pathway System (GePS) software (version 3.10; Intrexon Bioinformatics GmbH, Munich, Germany; settings: Orthologous genes from H. sapiens were used for this ranking, species bovine, analysed were proteins with ≥ 5-fold change). Further bioinformatic analyses were conducted with open source software ShinyGO v0.50: http://ge-lab.org/go/ (Ge and Jung, 2018), P-value cutoff (FDR) was set to 0.05.

3 Results

3.1. Differentially abundant proteins in secretomes and exoproteomes of PBL from control and immune deviant hosts as response to *in vitro* infection with MAP

We investigated the immune response of primary PBL isolated from control and immune deviant animals. After 48 hours of *in vitro* infection with live MAP, we harvested the mixed secretomes and exoproteomes of PBL and MAP and analysed them with mass spectrometry. Overall, we identified 826 proteins (811 bovine and 15 MAP proteins). Cluster analysis confirmed significant differences in protein abundances between PBL of control and ID cow in host-pathogen response (Figure 1, Venn diagramm). In secretome of control cow, 90 proteins were differentially upregulated (Figure 1, ≥ 5-fold change of expression, blue circle) in contrast to 38 proteins that were higher abundant in ID cow (Figure 1, light red circle). In the MAP exoproteome, although small in overall numbers, different protein abundances were also detectable. In MAP co-incubated with control PBL, one protein (GroEl1) was found with protein abundance change (Figure 2, blue circle; six-fold higher abundance) and one protein (DnaK) was upregulated in exoproteome after co-incubation with ID PBL (Figure 2, light red circle; 24-fold higher abundance).

3.2 Different biological pathways during the immune response in host PBL

Interpretation of large protein sets can be performed through enrichment analyses, using published information for examination of overrepresentation of a known set of genes within the input gene list (Ge and Jung, 2018; Merico et al., 2010). Since many gene ontology (GO) terms are related or redundant, we used a hierarchical clustering tree and network (ShinyGO v.050 (Ge and Jung, 2018)).

The top regulated biological process pathways in the secretome/excretome of the control were all related to RNA splicing (Figure 3A). The top regulated immune pathways were cellular immune responses of various leukocyte subsets, chemotaxis and the reaction to IL-12 (Figure 3A).

In contrast, in secretome/excretome of ID PBL, the top regulated pathways were response to stress and immune system process (Figure 3B). The enriched immune pathways comprised distinct routes of immune response in ID PBL, focussing on closely related positive regulations of cellular functions, complement activation and humoral immune response (Figure 3B). Visualization of network clearly indicates two major regulated networks in control PBL`s secretome (Figure 4A) and one distinct, major enriched network in ID proteins (Figure 4B).

3.3 GroEl1 and DnAK are differentially abundant in MAPs interacting with different hosts

Interestingly, there was also a clear difference in the regulated proteins of the pathogen itself, dependent on the co-cultivated host PBL (Table 1, supplementary table 2), although the low number of proteins was not sufficient for in depth enrichment analyses of the MAP exoproteomes. These differential proteome analyses clearly indicate substantial differences on protein level of the foodborne pathogen MAP in the interaction with different host immune capacities.

4 Discussion

Mycobacterium avium subsp. paratuberculosis (MAP) could be a foodborne pathogen, because it is discussed in association with several diseases (Cossu et al., 2019; Pierce, 2018; Sechi and Dow, 2015). MAP were found in patients with inflammatory bowel diseases like Crohn's disease and ulcerative colitis, as well as autoimmune diseases like type 1 diabetes, multiple sclerosis, rheumatoid arthritis and Hashimoto's thyroiditis (Garvey, 2018), but so far, a causal association has not yet been proven in any of these cases. Since MAP can survive many of the standard techniques of food decontamination (e.g. pasteurization), they are regularly found alive in pasteurized milk (Gerrard et al., 2018) and in dried dairy products such as powdered infant formula (Botsaris et al., 2016). If MAP play a role in pathogenesis of respective diseases, we think that this must be associated with a certain type of susceptibility from these hosts. MAP is ubiquitously found and only a minor proportion of consumers (if at all) is affected by MAP-associated diseases. The same is true for cows: while they are often in contact with MAP, resulting in high frequencies of seropositive animals – approximately 20% and at least 3–5% in several countries (Boelaert et al., 2000; Nielsen and Toft, 2009) – Johne`s disease incidence is very rare. For example, a total of 232 clinical cases of Johne`s disease were reported in Ireland from 1995 to 2002 (Kennedy et al., 2014), yielding an average annual rate of approximately 0.0005%, given a cattle population of six million (Maher et al., 2008). A study examining environmental samples from 362 dairy farms located in all 10 provinces of Canada for detection of MAP by culture revealed true prevalence estimates of 66% for farms in Western Canada, 54% in Ontario, 24% in Québec, and 47% in Atlantic Canada (Corbett et al., 2018).

From tuberculosis it is known that after infection with *Mycobacterium tuberculosis* (MTB), there is a 10% probability that the host will develop active tuberculosis and the bacterium may invade multiple organs (Zhai et al., 2019). Although 9 million new cases of active tuberculosis are still reported

annually, an estimated one-third of the world is infected with MTB while remaining asymptomatic, defined as latent TB (Dye et al., 1999). Among the individuals with latent TB, only 5–10% will develop active tuberculosis disease in course of their lifetime, because they effectively control the infection through their immune response (Dye et al., 1999). This immune response after MTB infection is highly complex as the bacteria have intricate immune escape mechanisms (Zhai et al., 2019).

For MAP, only little is known about host-pathogen reactions in general, and whether different immune responses exist, but a thorough examination of the respective mechanisms is of major importance to get functional data that allow a better understanding and a substantiated risk assessment. In the post-genomic era, proteomics represents a key discipline to perform in depth studies and identify the complex network of proteins involved in such host-bacteria communication. In this study, we analysed the exoproteomes/secretomes of MAP and host cow PBL with known, functionally different immune capacities (Lutterberg et al., 2018) using differential proteome analyses after *in vitro* infection. Interestingly, there were significant differences in protein abundances secreted from control and ID PBL. Ninety proteins were ≥ 5 fold higher abundant in control PBL after interaction with MAP. In the control, the top regulated immune pathways described cell activation and chemotaxis of leukocytes as well as IL-12 mediated signalling pathways. For *M. paratuberculosis* it was shown, that IL-12 transcription is increased in infected bovine macrophages within 6 hours (Weiss et al., 2002), probably to enhance the developing T cell response (Bannantine et al., 2015). To our knowledge, the role of IL-12 in MAP infections of cows has not been analysed so far, but the IL-12 associated immune response should also be protective. In tuberculosis it was shown that the induction of protective IFN-γ T cell responses against primary *M. tuberculosis* infection clearly depends on IL-12 (Khader et al., 2006). Mice lacking IL-12p40 cannot control the growth of the MTB bacterial infection (Cooper et al., 1997). These findings in mouse models were confirmed in man, where IL-12 was shown to be critical for preventing tuberculosis (Alcaïs et al., 2005). Therefore, we hypothesize that secretion of IL-12 from indicates a protective immune response against MAP infection in control PBL. In ID PBL on the other hand, CCR4-NOT transcription complex, subunit 1 (CNOT1) was detected as highly abundant protein (supplemental table 1). This novel finding of CNOT1 regulation in the bovine immune system is very interesting, because CCR4-NOT complex members have recently been shown to function as regulators ensuring repression of the MHCII locus in human cell lines (Rodríguez-Gil et al., 2017). Poor MHC II expression can cause autoimmune or infectious diseases, since MHCII is indispensable for adequate

immune responses (Rodríguez-Gil et al., 2017). Additionally, CNOT proteins also contribute to the downregulation of MHC class I gene expression by influencing transcription and mRNA degradation (Yang et al., 2016). Enriched network analyses of secreted proteins from ID PBL revealed further major different functions of the 38 differentially abundant proteins (Figure 4B). Members of complement activation pathway were enriched in ID PBL. We think the regulated candidates in ID PBL merit further investigation in future studies to clarify whether they indicate an immune response in favour of MAP infection or just another way to successfully fight mycobacterial infections.

Interestingly, in the MAP exoproteome (although small in overall numbers) different protein abundances were also detectable. Exoproteomes arise from cellular secretion, other protein export mechanisms or cell lysis, but only the most stable proteins in this environment will remain abundant (Armengaud et al., 2012). In MAP co-incubated with control PBL, GroEL1 showed 6-fold higher abundance. GroEL1 belongs to the family of 60 kDa heat shock proteins, also known as Cpn60s (GroELs) which are components of the essential protein folding machinery of the cell, but are also dominant antigens in many infectious diseases (Sharma et al., 2016). GroEL1 from MAP is highly immunogenic for cows (Yang et al., 2016). The exact function of GroEL1 in MAP is not clarified so far, but it is highly similar to the respective protein in MTB (Rv3417c), where GroEL1 is important for bacterial survival under low aeration by affecting the expression of genes known for hypoxia response (Sharma et al., 2016). From co-cultivation of MAP with ID PBL, on the other hand, DnaK emerged as differentially abundant protein. DnaK is a HSP70 family chaperone protein with essential function in stress induced protein refolding and DnaK loss is accompanied by disruption of membrane structure and increased cell permeability (Fay and Glickman, 2014). DnaK is essentially required for cell growth in mycobacteria due to a lack of redundancy with other chaperone systems (Fay and Glickman, 2014). This finding from MAP – ID PBL co-cultivation points to regulation of important survival mechanisms in MAP. However, these results must be interpreted with care because our analysed MAP exoproteome only comprised 15 proteins.

Conclusion:

Our data provide novel information about MAP-leukocyte interaction, adding to a more comprehensive picture of host-pathogen interactions. Co-incubation of MAP with cells from animals with different immune capacities led to significant differences in PBL secretomes and different immunological pathways enhanced in the hosts. In exoproteomes of respective MAPs, GroEL1 and DnaK were differentially abundant. These analyses gave a deeper insight into the different responses

of host PBL and MAP bacteria. In this study, several novel proteins were identified with changed abundance in host-pathogen interaction. These candidates merit further investigations in the future to clarify their functional role in infection control.

Author Contributions:

CD conceived and designed the experiments; KK, SH, KL, AS and CH performed the experiments; KK, SH, RD, EM and CD analyzed the data; CD wrote the manuscript. All authors critically read the manuscript and approved the final version to be published.

Conflict of interest:

The authors declare that the research was conducted in the absence of any commercial or financial relationships that could be construed as a potential conflict of interest.

Funding:

The IGF Project 18388 N of the FEI was supported via AiF within the program for promoting the Industrial Collective Research (IGF) of the German Ministry of Economic Affairs and Energy (BMWi), based on a resolution of the German Parliament.

Acknowledgements:

The authors would like to thank Barbara Amann for excellent technical support.

References

Kuenstner JT, Naser S, Chamberlin W, Borody T, Graham DY, McNees A, Hermon-Taylor J, Hermon-Taylor A, Dow CT, Thayer W, et al: The consensus from the Mycobacterium Avium Ssp. paratuberculosis (MAP) conference 2017. Front Public Health 2017;5:208.

Alcaïs, A., Fieschi, C., Abel, L., Casanova, J.-L., 2005. Tuberculosis in children and adults: two distinct genetic diseases. The Journal of Experimental Medicine 202, 1617-1621.

Alcedo, K.P., Thanigachalam, S., Naser, S.A., 2016. RHB-104 triple antibiotics combination in culture is bactericidal and should be effective for treatment of Crohn's disease associated with Mycobacterium paratuberculosis. Gut Pathogens 8, 32-32.

Armengaud, J., Christie-Oleza, J.A., Clair, G., Malard, V., Duport, C., 2012. Exoproteomics: exploring the world around biological systems. Expert Review of Proteomics 9, 561-575.

Bannantine, J.P., Stabel, J.R., Laws, E., D Cardieri, M.C., Souza, C.D., 2015. Mycobacterium avium Subspecies paratuberculosis Recombinant Proteins Modulate Antimycobacterial Functions of Bovine Macrophages. PLoS One 10, e0128966-e0128966.

Boelaert, F., Walravens, K., Biront, P., Vermeersch, J.P., Berkvens, D., Godfroid, J., 2000. Prevalence of paratuberculosis (Johne’s disease) in the Belgian cattle population. Veterinary Microbiology 77, 269-281.

Botsaris, G., Swift, B.M.C., Slana, I., Liapi, M., Christodoulou, M., Hatzitofi, M., Christodoulou, V., Rees, C.E.D., 2016. Detection of viable Mycobacterium avium subspecies paratuberculosis in powdered infant formula by phage-PCR and confirmed by culture. International Journal of Food Microbiology 216, 91-94.

Cooper, A.M., Magram, J., Ferrante, J., Orme, I.M., 1997. Interleukin 12 (IL-12) is crucial to the development of protective immunity in mice intravenously infected with mycobacterium tuberculosis. The Journal of Experimental Medicine 186, 39-45.

Corbett, C.S., Naqvi, S.A., Bauman, C.A., De Buck, J., Orsel, K., Uehlinger, F., Kelton, D.F., Barkema, H.W., 2018. Prevalence of Mycobacterium avium ssp. paratuberculosis infections in Canadian dairy herds. Journal of Dairy Science 101, 11218-11228.

Cossu, D., Yokoyama, K., Sakanishi, T., Momotani, E., Hattori, N., 2019. Adjuvant and antigenic properties of Mycobacterium avium subsp. paratuberculosis on experimental autoimmune encephalomyelitis. Journal of Neuroimmunology.

Davis, W.C., 2015. On deaf ears, Mycobacterium avium paratuberculosis in pathogenesis Crohn's and other diseases. World journal of gastroenterology 21, 13411-13417.

Dye, C., Scheele, S., Dolin, P., Pathania, V., Raviglione, M.C., for the, W.H.O.G.S., Monitoring, P., 1999. Global Burden of Tuberculosis: Estimated Incidence, Prevalence, and Mortality by Country. JAMA 282, 677-686.

Eslami, M., Shafiei, M., Ghasemian, A., Valizadeh, S., Al-Marzoqi, A.H., Shokouhi Mostafavi, S.K., Nojoomi, F., Mirforughi, S.A., 2019. Mycobacterium avium paratuberculosis and Mycobacterium avium complex and related subspecies as causative agents of zoonotic and occupational diseases. Journal of Cellular Physiology 0.

Fay, A., Glickman, M.S., 2014. An essential nonredundant role for mycobacterial DnaK in native protein folding. PLoS Genet 10, e1004516-e1004516.

Ge, S., Jung, D., 2018. ShinyGO: a graphical enrichment tool for animals and plants. bioRxiv, 315150.

Gerrard, Z.E., Swift, B.M.C., Botsaris, G., Davidson, R.S., Hutchings, M.R., Huxley, J.N., Rees, C.E.D., 2018. Survival of Mycobacterium avium subspecies paratuberculosis in retail pasteurised milk. Food Microbiology 74, 57-63.

Grosche, A., Hauser, A., Lepper, M.F., Mayo, R., von Toerne, C., Merl-Pham, J., Hauck, S.M., 2016. The Proteome of Native Adult Müller Glial Cells From Murine Retina. Mol Cell Proteomics 15, 462-480.

Guo, M.S., Gross, C.A., 2014. Stress-induced remodeling of the bacterial proteome. Curr Biol 24, R424-R434.

Hauck, S.M., Hofmaier, F., Dietter, J., Swadzba, M.E., Blindert, M., Amann, B., Behler, J., Kremmer, E., Ueffing, M., Deeg, C.A., 2012. Label-free LC-MSMS analysis of vitreous from autoimmune uveitis reveals a significant decrease in secreted Wnt signalling inhibitors DKK3 and SFRP2. J Proteomics 75, 4545-4554.

Hauck, S.M., Lepper, M.F., Hertl, M., Sekundo, W., Deeg, C.A., 2017. Proteome Dynamics in Biobanked Horse Peripheral Blood Derived Lymphocytes (PBL) with Induced Autoimmune Uveitis. PROTEOMICS 17, 1700013.

Hermon-Taylor, J., 2000. Mycobacterium avium subspecies paratuberculosis in the causation of Crohn's disease. World journal of gastroenterology 6, 630-632.

Hobmaier, B.F., Lutterberg, K., Kleinwort, K.J.H., Mayer, R., Hirmer, S., Amann, B., Hölzel, C., Märtlbauer, E.P., Deeg, C.A., 2019. Characterization of plant lectins for their ability to isolate Mycobacterium avium subsp. paratuberculosis from milk. Food Microbiology 82, 231-239.

Kennedy, A.E., Da Silva, A.T., Byrne, N., Govender, R., MacSharry, J., O'Mahony, J., Sayers, R.G., 2014. The Single Intradermal Cervical Comparative Test Interferes with Johne's Disease ELISA Diagnostics. Frontiers in Immunology 5, 564-564.

Khader, S.A., Partida-Sanchez, S., Bell, G., Jelley-Gibbs, D.M., Swain, S., Pearl, J.E., Ghilardi, N., Desauvage, F.J., Lund, F.E., Cooper, A.M., 2006. Interleukin 12p40 is required for dendritic cell migration and T cell priming after Mycobacterium tuberculosis infection. The Journal of Experimental Medicine 203, 1805-1815.

Kuenstner, J.T., Naser, S., Chamberlin, W., Borody, T., Graham, D.Y., McNees, A., Hermon-Taylor, J., Hermon-Taylor, A., Dow, C.T., Thayer, W., Biesecker, J., Collins, M.T., Sechi, L.A., Singh, S.V., Zhang, P., Shafran, I., Weg, S., Telega, G., Rothstein, R., Oken, H., Schimpff, S., Bach, H., Bull, T., Grant, I., Ellingson, J., Dahmen, H., Lipton, J., Gupta, S., Chaubey, K., Singh, M., Agarwal, P., Kumar, A., Misri, J., Sohal, J., Dhama, K., Hemati, Z., Davis, W., Hier, M., Aitken, J., Pierce, E., Parrish, N., Goldberg, N., Kali, M., Bendre, S., Agrawal, G., Baldassano, R., Linn, P., Sweeney, R.W., Fecteau, M., Hofstaedter, C., Potula, R., Timofeeva, O., Geier, S., John, K., Zayanni, N., Malaty, H.M., Kahlenborn, C., Kravitz, A., Bulfon, A., Daskalopoulos, G., Mitchell, H., Neilan, B., Timms, V., Cossu, D., Mameli, G., Angermeier, P., Jelic, T., Goethe, R., Juste, R.A., Kuenstner, L., 2017. The Consensus from the Mycobacterium avium ssp. paratuberculosis (MAP) Conference 2017. Frontiers in public health 5, 208-208.

Li, L., Bannantine, J.P., Campo, J.J., Randall, A., Grohn, Y.T., Katani, R., Schilling, M., Radzio-Basu, J., Kapur, V., 2017. Identification of sero-reactive antigens for the early diagnosis of Johne's disease in cattle. PLoS One 12, e0184373.

Li, L., Katani, R., Schilling, M., Kapur, V., 2016. Molecular Epidemiology of Mycobacterium avium subsp. paratuberculosis on Dairy Farms. Annual Review of Animal Biosciences 4, 155-176.

Lutterberg, K., Kleinwort, K.J.H., Hobmaier, B.F., Hauck, S.M., Nüske, S., Scholz, A.M., Deeg, C.A., 2018. A Functionally Different Immune Phenotype in Cattle Is Associated With Higher Mastitis Incidence. Frontiers in Immunology 9, 2884-2884.

Machado, G., Kanankege, K., Schumann, V., Wells, S., Perez, A., Alvarez, J., 2018. Identifying individual animal factors associated with Mycobacterium avium subsp. paratuberculosis (MAP) milk ELISA positivity in dairy cattle in the Midwest region of the United States. BMC Veterinary Research 14, 28.

Maher, P., Good, M., More, S., 2008. Trends in cow numbers and culling rate in the Irish cattle population, 2003 to 2006. Irish veterinary journal 61, 455-463.

Mendoza, J.L., Lana, R., Díaz-Rubio, M., 2009. Mycobacterium avium subspecies paratuberculosis and its relationship with Crohn's disease. World journal of gastroenterology 15, 417-422.

Merico, D., Isserlin, R., Stueker, O., Emili, A., Bader, G.D., 2010. Enrichment Map: A Network-Based Method for Gene-Set Enrichment Visualization and Interpretation. PLoS One 5, e13984.

Nielsen, S.S., Toft, N., 2009. A review of prevalences of paratuberculosis in farmed animals in Europe. Preventive Veterinary Medicine 88, 1-14.

Pierce, E.S., 2018. Could Mycobacterium avium subspecies paratuberculosis cause Crohn’s disease, ulcerative colitis…and colorectal cancer? Infectious Agents and Cancer 13, 1.

Rodríguez-Gil, A., Ritter, O., Saul, V.V., Wilhelm, J., Yang, C.-Y., Grosschedl, R., Imai, Y., Kuba, K., Kracht, M., Schmitz, M.L., 2017. The CCR4-NOT complex contributes to repression of Major Histocompatibility Complex class II transcription. Scientific Reports 7, 3547-3547.

Rubiano-Labrador, C., Bland, C., Miotello, G., Armengaud, J., Baena, S., 2015. Salt Stress Induced Changes in the Exoproteome of the Halotolerant Bacterium Tistlia consotensis Deciphered by Proteogenomics. PLoS One 10, e0135065-e0135065.

Sechi, L.A., Dow, C.T., 2015. Mycobacterium avium ss. paratuberculosis Zoonosis – The Hundred Year War – Beyond Crohn’s Disease. Frontiers in Immunology 6.

Sergeant, E.S.G., McAloon, C.G., Tratalos, J.A., Citer, L.R., Graham, D.A., More, S.J., 2019. Evaluation of national surveillance methods for detection of Irish dairy herds infected with Mycobacterium avium ssp. paratuberculosis. Journal of Dairy Science 102, 2525-2538.

Sharma, A., Rustad, T., Mahajan, G., Kumar, A., Rao, K.V.S., Banerjee, S., Sherman, D.R., Mande, S.C., 2016. Towards understanding the biological function of the unusual chaperonin Cpn60.1 (GroEL1) of Mycobacterium tuberculosis. Tuberculosis 97, 137-146.

Sweeney, R.W., 2011. Pathogenesis of Paratuberculosis. Veterinary Clinics of North America: Food Animal Practice 27, 537-546.

Weiss, D.J., Evanson, O.A., Moritz, A., Deng, M.Q., Abrahamsen, M.S., 2002. Differential responses of bovine macrophages to Mycobacterium avium subsp. paratuberculosis and Mycobacterium avium subsp. avium. Infection and Immunity 70, 5556-5561.

Yamamoto, T., Murai, K., Hayama, Y., Kobayashi, S., Nagata, R., Kawaji, S., Osaki, M., Sakakibara, S.-i., Tsutsui, T., 2018. Evaluation of fecal shedding and antibody response in dairy cattle infected with paratuberculosis using national surveillance data in Japan. Preventive Veterinary Medicine 149, 38-46.

Yang, C.-Y., Ramamoorthy, S., Boller, S., Rosenbaum, M., Rodriguez Gil, A., Mittler, G., Imai, Y., Kuba, K., Grosschedl, R., 2016. Interaction of CCR4–NOT with EBF1 regulates gene-specific transcription and mRNA stability in B lymphopoiesis. Genes & Development 30, 2310-2324.

Zhai, W., Wu, F., Zhang, Y., Fu, Y., Liu, Z., 2019. The Immune Escape Mechanisms of Mycobacterium Tuberculosis. International Journal of Molecular Sciences 20, 340.

Captions for figures:

Figure 1: Overlap (Venn diagram) of differentially (≥ 5 fold) expressed proteins between secretomes/exoproteomes of control cow (blue) and ID cow (red). From a total of 811 identified proteins, 90 were higher abundant in control and 38 in ID.

Figure 2: Overlap (Venn diagram) of differentially (≥ 5 fold) expressed proteins between exoproteomes of MAP co-incubated with PBL of control cow (blue) and MAP co-incubated with PBL of ID cow (red). From a total of 15 identified proteins, one different protein from each specimen showed higher abundance.

Figure 3: Hierarchical clustering tree and network of related GO terms of differentially expressed proteins in secretomes/exoproteomes of control PBL (A) and ID PBL (B) illustrates marked differences. GO terms are grouped together based on how many genes they share. The size of the solid circle corresponds to the enrichment false discovery rate.

Figure 4: Visualization of overlapping relationships among enriched gene-sets revealed A) two major networks as shown by network view for enriched GO molecular component terms in control PBL after MAP infection and B) in ID PBL after MAP infection. Related GO terms are connected by a line whose thickness reflects percent of overlapping genes. Size of the nodes corresponds to number of genes.

Tables:

Table 1. Regulation of MAP proteins identified in secretomes/exoproteomes after co-incubation with control and ID PBL.

	Accession	**Gene symbol**	**Description**	**Ratio MAP Ctr/ID**
1	AAS06815	GroEL1	pep:novel chromosome:GCA_000007865.1:Chromosome:4733338:4734954:1 gene:MAP_4265 transcript:AAS06815 description:""GroEL1""	6,07
2	ETB04387	F0F1 ATP synthase subunit alpha	pep:novel supercontig:GCA_000504785.1:contig000131:9486:11150:1 gene:O979_07265 transcript:ETB04387 description:""F0F1 ATP synthase subunit alpha""	3,26
3	ETB05569	DNA-binding protein	pep:novel supercontig:GCA_000504785.1:contig000072:8572:9225:1 gene:O979_04085 transcript:ETB05569 description:""DNA-binding protein""	2,47
4	AAS06727	RplN	pep:novel chromosome:GCA_000007865.1:Chromosome:4652017:4652385:1 gene:MAP_4177 transcript:AAS06727 description:""RplN""	2,34
5	AAS06486; ELP44387; ETB08817	GroEL2	pep:novel chromosome:GCA_000007865.1:Chromosome:4395922:4397547:1 gene:MAP_3936 transcript:AAS06486 description:""GroEL2""	1,12
6	AAS06693	Tuf	pep:novel chromosome:GCA_000007865.1:Chromosome:4620946:4622136:1 gene:MAP_4143 transcript:AAS06693 description:""Tuf""	0,88
7	ETB02420	enoyl-CoA hydratase	pep:novel supercontig:GCA_000504785.1:contig000238:14619:15410:1 gene:O979_11400 transcript:ETB02420 description:""enoyl-CoA hydratase""	0,86

8	ETB00930	2-isopropyl malate synthase	pep:novel supercontig:GCA_000504845.1:contig000411:16560:18359:-1 gene:O978_19245 transcript:ETB00930 description:""2-isopropylmalate synthase""	0,75
9	AAS06690	RpsL	pep:novel chromosome:GCA_000007865.1:Chromosome:4617754:4618128:1 gene:MAP_4140 transcript:AAS06690 description:""RpsL""	0,67
10	AAS06681; ETB45918; ETB45924	RpoC	pep:novel chromosome:GCA_000007865.1:Chromosome:4606729:4610679:1 gene:MAP_4131 transcript:AAS06681 description:""RpoC""	0,62
11	AAS06680	RpoB	pep:novel chromosome:GCA_000007865.1:Chromosome:4603087:4606683:1 gene:MAP_4130 transcript:AAS06680 description:""RpoB""	0,48
12	AAS02778	ClpC	pep:novel chromosome:GCA_000007865.1:Chromosome:488298:490829:1 gene:MAP_0461 transcript:AAS02778 description:""ClpC""	0,46
13	ETB04840	GTP-binding protein YchF	pep:novel supercontig:GCA_000504785.1:contig000104:1736:2809:1 gene:O979_06015 transcript:ETB04840 description:""GTP-binding protein YchF""	0,43
14	ETB04389 AAS04768	ATP synthase subunit beta	pep:novel supercontig:GCA_000504785.1:contig000131:12100:13557:1 gene:O979_07275 transcript:ETB04389 description:""ATP synthase subunit beta""	0,26
15	AAS06390	DnaK	pep:novel chromosome:GCA_000007865.1:Chromosome:4295544:4297415:1 gene:MAP_3840 transcript:AAS06390 description:""DnaK""	0,04

Captions for supplementary material:

Supplementary table 1: All proteins identified in PBL secretome analyses of co-cultivation of MAP with PBL from donors with different immune capacities.

Supplementary table 2: All proteins identified in MAP exoproteome analyses of co-cultivation of MAP with PBL from donors with different immune capacities.

Data Availability Statement:

The datasets generated and analyzed for this study are available in supplemental tables 1 and 2.

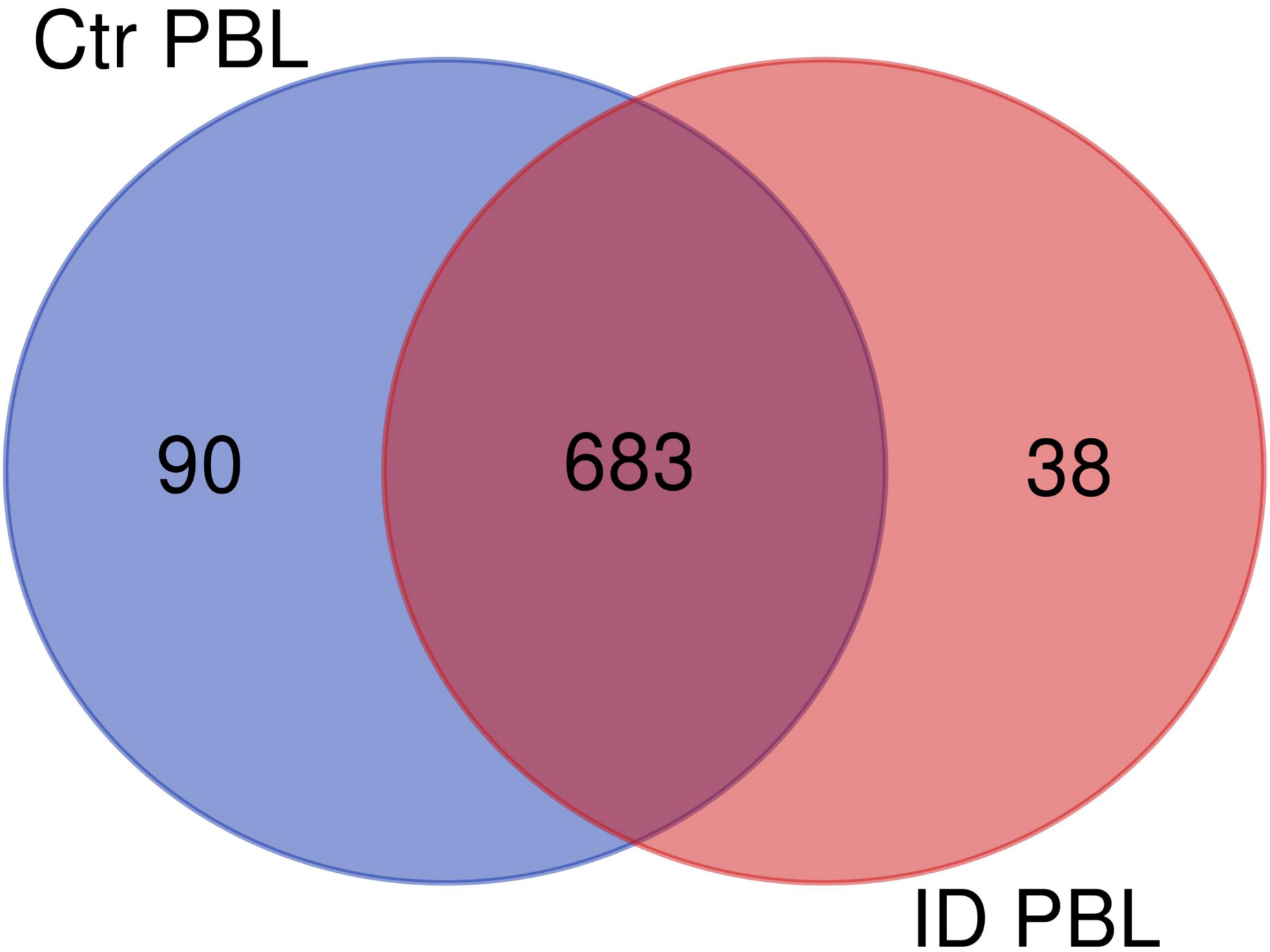
Ctr PBL
90
683
38
ID PBL

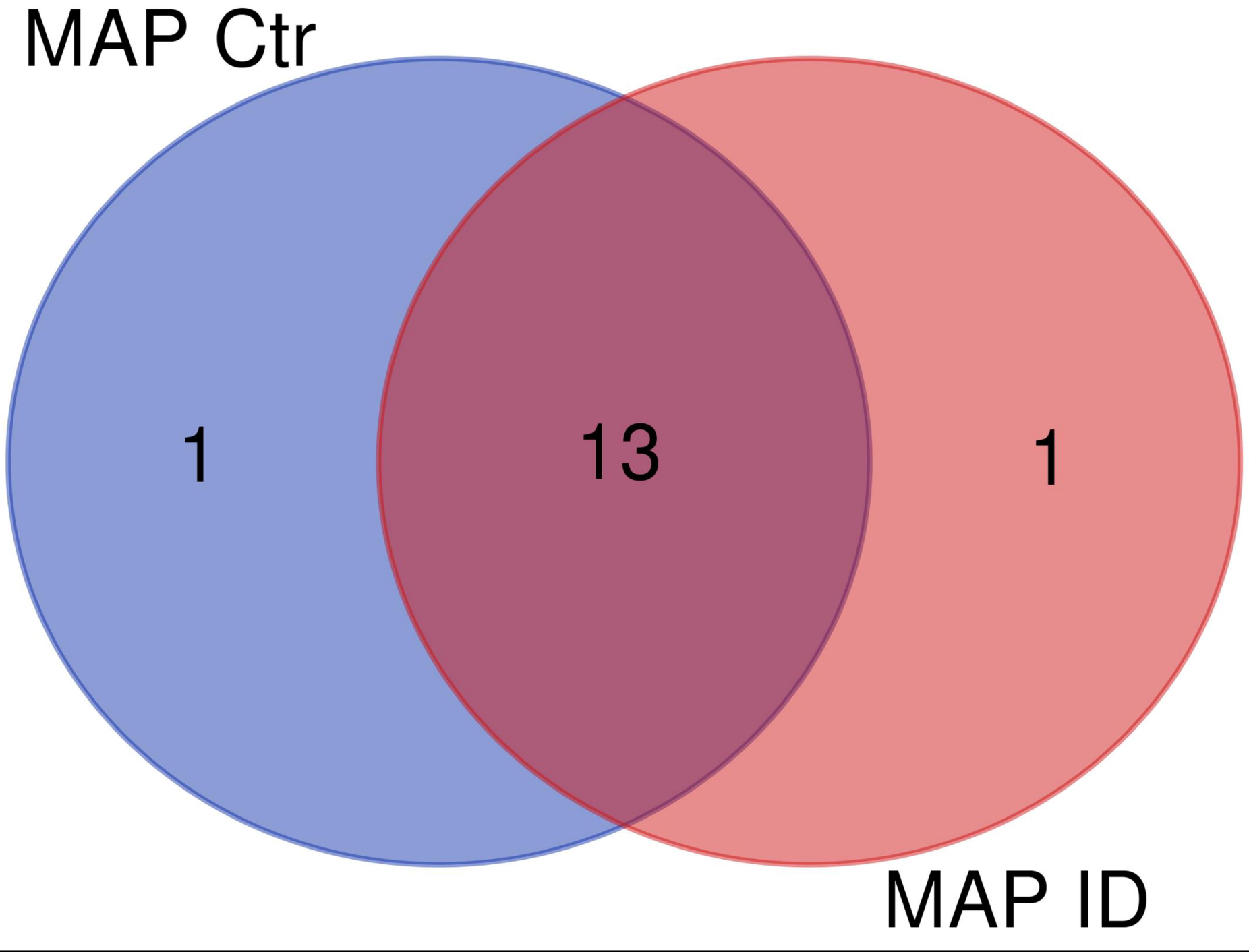
MAP Ctr
1
13
1
MAP ID

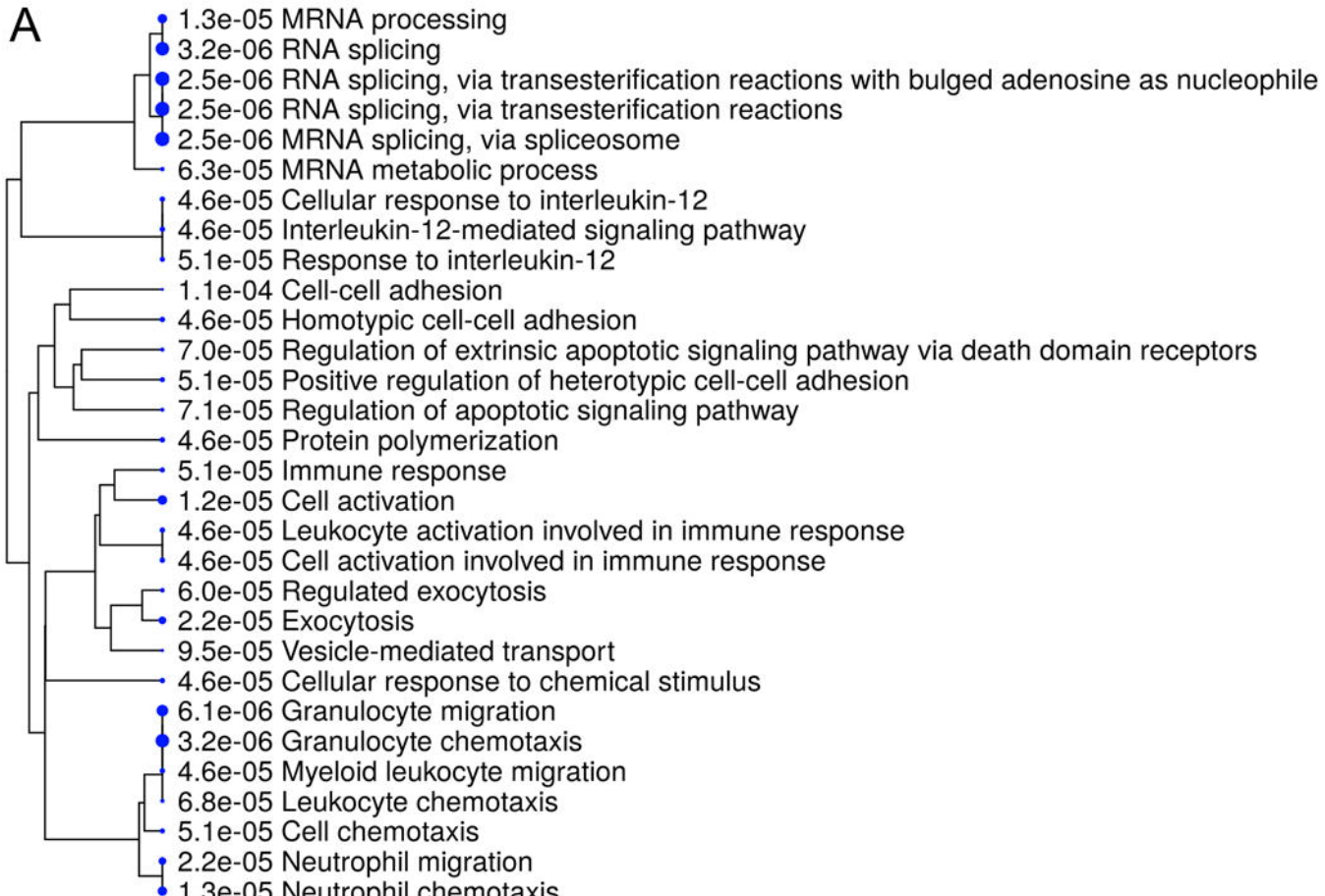
A
1.3e-05 MRNA processing
3.2e-06 RNA splicing
2.5e-06 RNA splicing, via transesterification reactions with bulged adenosine as nucleophile
2.5e-06 RNA splicing, via transesterification reactions
2.5e-06 MRNA splicing, via spliceosome
6.3e-05 MRNA metabolic process
4.6e-05 Cellular response to interleukin-12
4.6e-05 Interleukin-12-mediated signaling pathway
5.1e-05 Response to interleukin-12
1.1e-04 Cell-cell adhesion
4.6e-05 Homotypic cell-cell adhesion
7.0e-05 Regulation of extrinsic apoptotic signaling pathway via death domain receptors
5.1e-05 Positive regulation of heterotypic cell-cell adhesion
7.1e-05 Regulation of apoptotic signaling pathway
4.6e-05 Protein polymerization
5.1e-05 Immune response
1.2e-05 Cell activation
4.6e-05 Leukocyte activation involved in immune response
4.6e-05 Cell activation involved in immune response
6.0e-05 Regulated exocytosis
2.2e-05 Exocytosis
9.5e-05 Vesicle-mediated transport
4.6e-05 Cellular response to chemical stimulus
6.1e-06 Granulocyte migration
3.2e-06 Granulocyte chemotaxis
4.6e-05 Myeloid leukocyte migration
6.8e-05 Leukocyte chemotaxis
5.1e-05 Cell chemotaxis
2.2e-05 Neutrophil migration
1.3e-05 Neutrophil chemotaxis

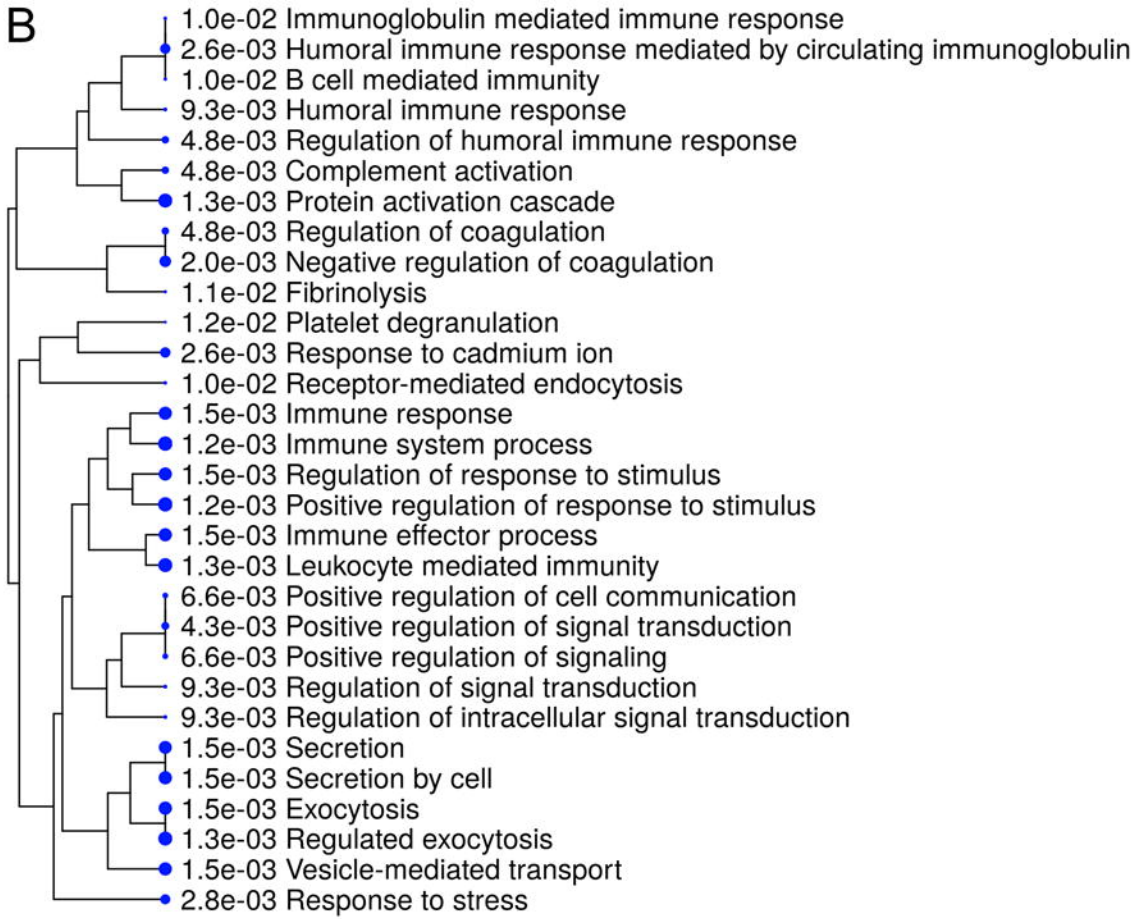
B
1.0e-02 Immunoglobulin mediated immune response
2.6e-03 Humoral immune response mediated by circulating immunoglobulin
1.0e-02 B cell mediated immunity
9.3e-03 Humoral immune response
4.8e-03 Regulation of humoral immune response
4.8e-03 Complement activation
1.3e-03 Protein activation cascade
4.8e-03 Regulation of coagulation
2.0e-03 Negative regulation of coagulation
1.1e-02 Fibrinolysis
1.2e-02 Platelet degranulation
2.6e-03 Response to cadmium ion
1.0e-02 Receptor-mediated endocytosis
1.5e-03 Immune response
1.2e-03 Immune system process
1.5e-03 Regulation of response to stimulus
1.2e-03 Positive regulation of response to stimulus
1.5e-03 Immune effector process
1.3e-03 Leukocyte mediated immunity
6.6e-03 Positive regulation of cell communication
4.3e-03 Positive regulation of signal transduction
6.6e-03 Positive regulation of signaling
9.3e-03 Regulation of signal transduction
9.3e-03 Regulation of intracellular signal transduction
1.5e-03 Secretion
1.5e-03 Secretion by cell
1.5e-03 Exocytosis
1.3e-03 Regulated exocytosis
1.5e-03 Vesicle-mediated transport
2.8e-03 Response to stress

A
MRNA processing
RNA splicing, via transesterification reactions
RNA splicing
MRNA splicing, via spliceosome
MRNA metabolic process
RNA splicing, via transesterification reactions with bulged adenosine as nucleophile
Cellular response to chemical stimulus
Response to interleukin-12
Interleukin-12-mediated signaling pa
Cellular response to interleukin-12
Myeloid leukocyte migration
Leukocyte chemotaxis
Exocytosis
Cell activation involved in immune response
Vesicle-mediated transport
Cell-cell adhesion
Granulocyte migration
Homotypic cell-cell adhesion
Cell activation
Leukocyte activation involved in immune response
Regulation of apoptotic signaling pathway
Granulocyte chemotaxis
Neutrophil migration
Immune response
Positive regulation of heterotypic cell-cell adhesion
Neutrophil chemotaxis
Regulated exocytosis
Chemotaxis
Regulation of extrinsic apoptotic signaling pathway via death domain receptors
Protein polymerization

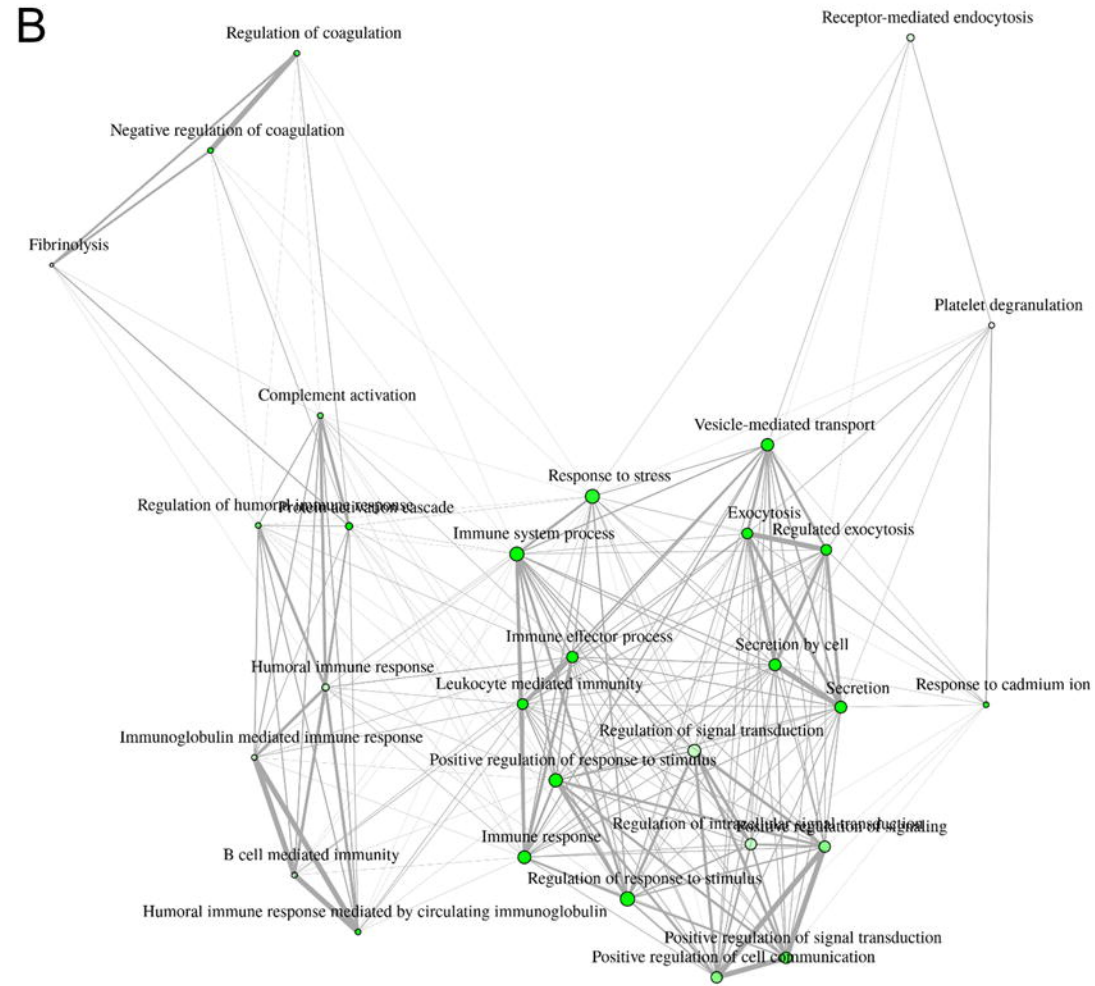
B
Regulation of coagulation
Receptor-mediated endocytosis
Negative regulation of coagulation
Fibrinolysis
Platelet degranulation
Complement activation
Vesicle-mediated transport
Response to stress
Regulation of humoral immune response
Proteolysis
Complement cascade
Exocytosis
Immune system process
Regulated exocytosis
Immune effector process
Secretion by cell
Humoral immune response
Leukocyte mediated immunity
Secretion
Response to cadmium ion
Immunoglobulin mediated immune response
Regulation of signal transduction
Positive regulation of response to stimulus
Regulation of intracellular signal transduction
Positive regulation of signaling
Immune response
B cell mediated immunity
Regulation of response to stimulus
Humoral immune response mediated by circulating immunoglobulin
Positive regulation of signal transduction
Positive regulation of cell communication